

# EFFICIENT LINEAR AND NONLINEAR SEISMIC SSI ANALYSIS OF DEEPLY EMBEDDED STRUCTURES USING FLEXIBLE VOLUME REDUCED-ORDER MODELING (FVROM)

Dan M. Ghiocel

President, Ghiocel Predictive Technologies, Inc., New York (dan.ghiocel@ghiocel-tech.com)

## ABSTRACT

The paper introduces and illustrates the application of a highly efficient approach for performing seismic SSI analysis of deeply embedded structures. The approach bases on the SSI analysis performed by Flexible Volume Substructuring (FVS) in complex frequency domain, also known as SASSI methodology. The Flexible Volume Reduced-Order Modeling (FVROM) approach presented herein is a “theoretically exact” approach implemented in the ACS SASSI software based on the condensation of the excavated soil impedance matrix at the foundation-soil interface nodes. The FVROM approach efficiency is further improved using a fast interpolation scheme for the condensed soil matrix. This higher numerical efficiency implementation is called the FVROM-INT (FVROM with INTERpolation) approach, and drastically reduces the overall SSI analysis computational effort in comparison with the reference SASSI Flexible Volume (FV) approach. Using the FVROM-INT approach, the paper investigates the dynamic behavior of two deeply embedded structures: 1) AB shearwall structure, and 2) typical SMR structure. Both linear and nonlinear structure SSI analyses were performed. The presented results provide useful insights for a better understanding of deeply embedded SMR behavior under severe earthquakes.

## THEORETICAL BACKGROUND

The FVROM concept implemented in the ACS SASSI code (GP Technologies, 2021) is similar with the Soil Library concept currently used for the NuScale SMR seismic SSI analysis using the ANSYS code (Mertz et al., 2019). The Soil Library concept is implemented in ACS SASSI Option AA-R (for Advanced-ANSYS solution with Reduced soil impedance) for optionally performing linear seismic SSI analysis with ANSYS in the complex frequency domain (ANSYS, 2019).

Using FVS approach, the dynamic SSI solution is computed for the coupled structure-excavated soil system defined in complex frequency. In the original SASSI FVS implementation the coupled SSI system is partitioned into three coupled dynamic subsystems, namely, the infinite free-field soil system, the structural system, and the excavated soil system (Lysmer et al., 1981). The FE modeling consists of two coupled 3DFEM models which include the structural system and the excavated soil system, while the infinite soil system is idealized by its frequency-dependent impedance function. Since the structure and the excavated soil 3DFEM models are a part of the same SSI model they should be mesh-compatible at the foundation-soil interface. The reference SASSI FV method is a “theoretically exact” method. The reference FV method “interaction nodes” which ensure the compatibility between the excavation volume and the free-field soil motions include all excavated volume soil nodes (each node with three translations for the soil motion).

The FVROM SSI approach implemented in the ACS SASSI V4 software (GP Technologies, 2021) uses the condensation of the excavated soil impedance matrix  $\mathbf{Z}(\omega)$  at the foundation-soil interface nodes (the other excavation internal nodes and ground surface nodes are eliminated). The excavated soil matrix  $\mathbf{Z}(\omega)$  is computed based on the the soil layering impedance matrix and the excavated soil dynamic matrix, i.e.  $\mathbf{Z}(\omega) = \mathbf{X}(\omega) - \mathbf{C}^e(\omega)$  at each SSI frequency. The SSI system response is obtained using FVROM using the reduced-size excavated soil impedance matrix  $\tilde{\mathbf{Z}}_{ii}(\omega)$  and the associated reduced-size load vector  $\{\tilde{\mathbf{F}}_i(\omega)\}$  at each SSI frequency.

The SSI system equation becomes for the reduced-size SSI system:

$$\begin{aligned} ([\mathbf{C}_{ii}^s] + \tilde{\mathbf{Z}}_{ii})\{\mathbf{U}_i\} + [\mathbf{C}_{is}^s]\{\mathbf{U}_s\} &= \{\tilde{\mathbf{F}}_i\} \\ [\mathbf{C}_{si}^s]\{\mathbf{U}_i\} + [\mathbf{C}_{ss}^s]\{\mathbf{U}_s\} &= \{\mathbf{0}\} \end{aligned} \quad (1)$$

where  $[\mathbf{C}^s]$  and  $\{\mathbf{U}_s\}$  are the structure dynamic stiffness and the complex displacement solution. Indices s and i correspond to structure and soil interface degrees of freedom, respectively. It should be noted that FVROM approach based on excavation impedance condensation is a “theoretically exact” approach.

The FVROM matrix condensation can be further combined with an efficient interpolation of the reduced-size soil impedance matrix in complex frequency. Such an approach which combines matrix condensation with fast interpolation is named FVROM-INT (FVROM with INTerpolation). Since the excavated soil impedance variation in frequency is much smoother than the SSI response variation, interpolating it is highly efficient for speeding up the overall computational effort of SSI analysis. Only a reduced number of frequencies can be used for accurately computing the condensed soil impedance matrix and seismic load vector, and then, interpolating them for the rest of all other SSI frequencies.

### ACS SASSI IMPLEMENTATION

For a practical implementation of the FVROM-INT approach a reduced number of condensation frequencies of about 15-20 are usually sufficient for an accurate interpolation of the soil impedance interpolation. After the SSI response is computed, say for 100-200 SSI frequencies, this response is further interpolated for all Fourier frequencies used for describing the input motion data in the frequency domain which may include 8,192, 16,384 or 32,768 frequencies, or even a larger number.

It should be noted that the FVROM-INT approach implementation can be used in conjunction with the “exact” FV method, but also other “approximate” methods as the different options of the Extended Subtraction Method (ESM) which are acceptable in practice. For latter case, the solution approximations inherent to the ESM method for the full-size SSI system are transmitted to the reduced-size SSI system.

The FVROM-INT implementation has three computational steps described below, and in Figure 1:

- 1) Identify key or condensation frequencies based on free-field analysis results
- 2) Compute condensed excavation impedance matrix and seismic load vector for key frequencies, and interpolate excavation impedance matrix and seismic load vector for all SSI frequencies
- 3) Compute SSI system solution using the reduced excavation impedance matrix and load vectors

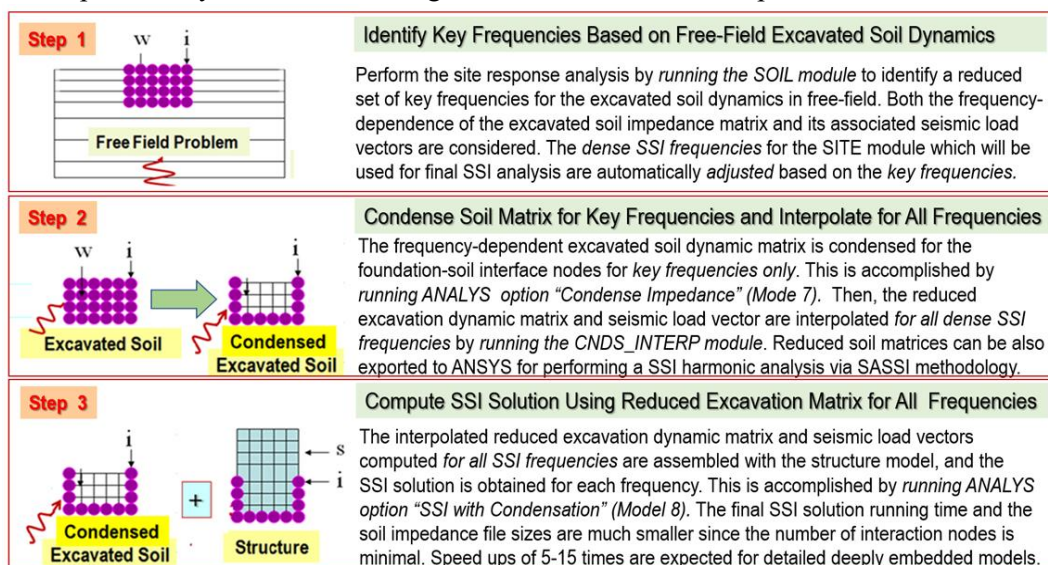


Figure 1. ACS SASSI V4 FVROM-INT SSI Approach for Deeply Embedded Structures

Step 1 is performed via the SOIL module, while steps 2 and 3 are performed using the ANALYS module in Mode 7 and Mode 8, also including the CDNS\_MTX\_INTERP module.

## DEEPLY EMBEDDED STRUCTURE CASE STUDIES

This section shows the application of the FVROM-INT approach for two SSI case studies: 1) AB Shearwall Structure and 2) A Typical SMR structure. Different soil layering cases, including uniform and nonuniform soils are considered, since the excavation impedance matrix variation in frequency is sensitive to soil layering nonuniformity. Both linear and nonlinear SSI analysis were performed using a hybrid frequency-time domain approach.

### *Auxiliary Building (AB) Shearwall Structure*

The AB structure SSI model shown in Figure 2 has a plan size 92m x 46m and a height of 46.6m with 30.3m above ground surface and 16.3m below ground surface. The soil site is described by a deep uniform soil with  $V_s = 1000$  fps. The seismic input is defined at foundation level. The SSI model includes 12,298 interaction nodes in the excavated soil part for the standard SASSI FV method, but only 2,458 condensed interaction nodes at the foundation-interface. To apply the FVROM-INT approach, preliminarily the condensation or key frequencies need to be determined by performing a free-field soil response analysis using the SOIL module. Only 22 key frequencies were determined for the entire SSI frequency range from 0 to 40 Hz. Figure 3 shows the acceleration transfer function (ATF) amplitudes computed using the reference FV method (“Direct SSI”) and the FVROM-INT approach (“Condensation with Interpolation”) for two locations as indicated in Figure 2. The computed ATF plots using the FVROM-INT approach and the reference FV method completely overlap. The key frequencies are shown with circle markers.

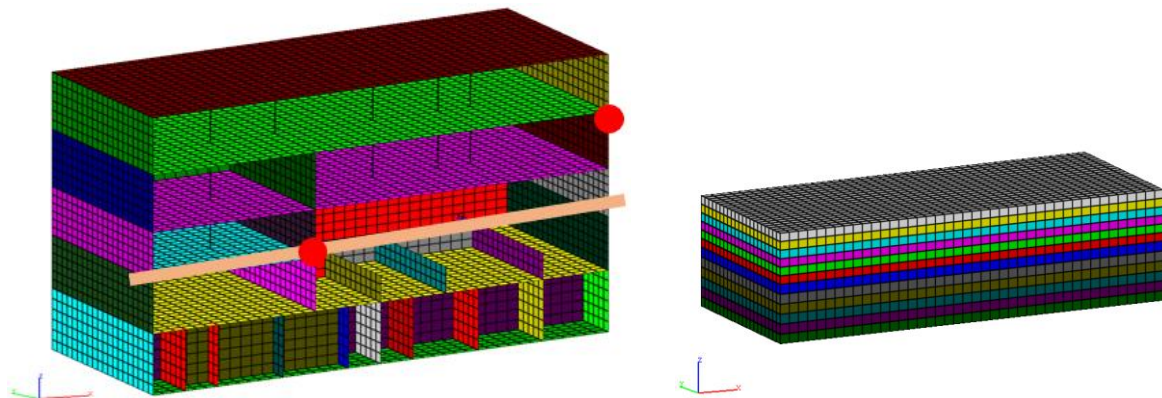


Figure 2 AB Structure SSI Model; Structure Model (left) and Excavated Soil Model (right)

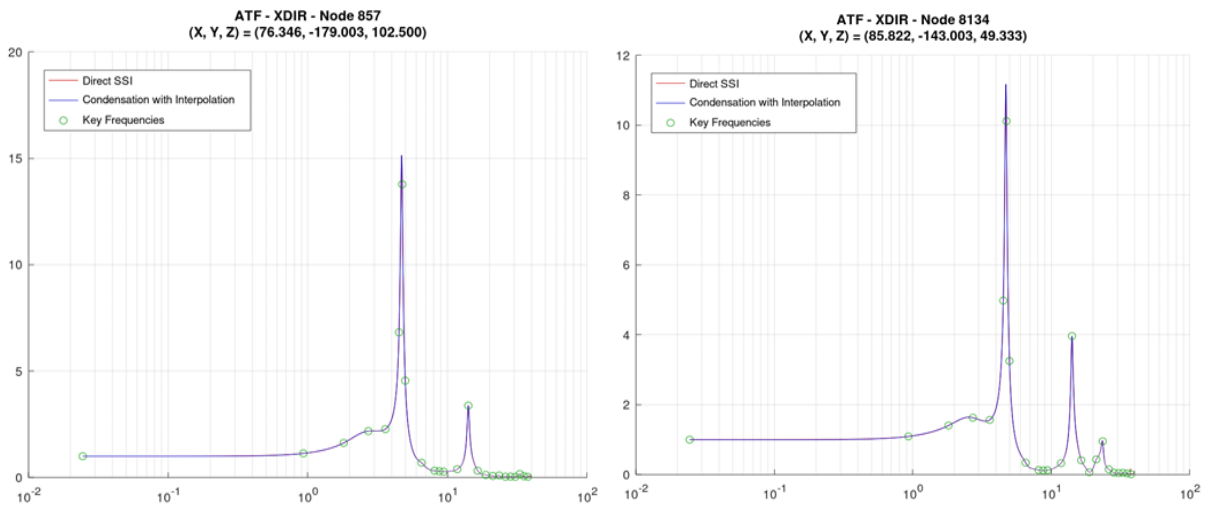


Figure 3 Computed ATF Amplitudes at Two Locations at Ground Surface (left) and Above (right)

The overall SSI analysis run speed-up obtained by FVROM-INT vs. reference FV method (12, 298 interaction nodes) was more than 8.5 times for the same computer platform. It should be noted that the FVROM-INT approach is even more efficient, by more than one magnitude order than the FV method, for nonlinear structure SSI analyses based on an iterative equivalent-linear SSI algorithm as implemented in ACS SASSI Option NON (for NONlinear RC structure modeling). Overall, the nonlinear SSI analysis using FVROM-INT took only about twice runtime than the linear SSI analysis.

It should be noted that the ACS SASSI Option NON was developed in compliance with the US and Japan standards for nonlinear modeling of the RC structures (Ghiocel et al. 2022 a, b). Independent verification and validation studies against NUPEC experimental testing and sophisticated nonlinear time domain analysis (based IAEA KARISMA project) indicated that the iterative SSI equivalent-linearization procedure implemented in the ACS SASSI Option NON provides a reasonable accuracy and a high numerical efficiency (Ichihara et al., 2021, 2022).

Figure 4 shows the nonlinear hysteretic shear force response in the internal transverse RC wall at the 2<sup>nd</sup> floor level (see Figure 2 for the wall location, with Panel 21 being at lower floor level) consistent with the ACI 318-19 and ASCE 4-16 recommendations for the RC wall modeling.

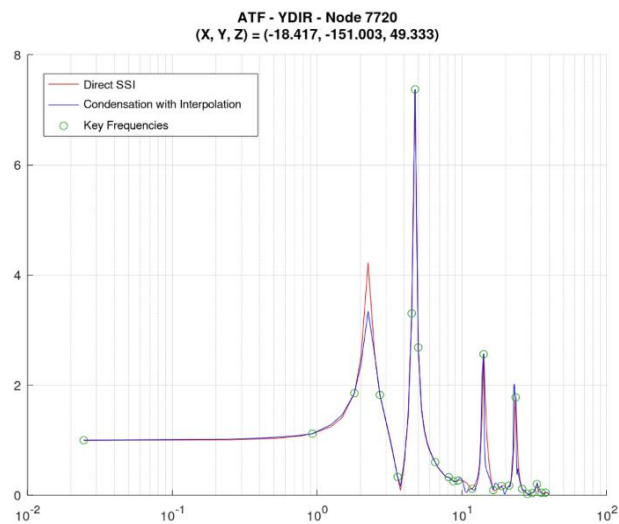
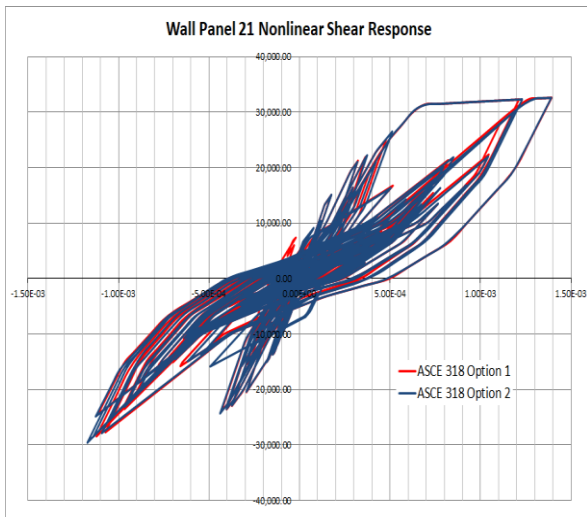


Figure 4. Nonlinear Response in Transverse Wall      Figure 5 Comparative ATF at the 2<sup>nd</sup> Floor Level

It should be also noted that for highly nonuniform soils, the soil impedance frequency variation is much sharper than for uniform soils, and therefore, there is a chance that some condensation frequencies could be missed. This can happen for condensation frequencies lower than the embedment layer fundamental frequency. To ensure that the automatically identified key frequencies based on the free-field analysis provide an accurate SSI solution, the analyst, after SSI analysis is completed, should check the computed ATF (.TFU files) curves for few structural locations against the key frequency data. If there is a significant ATF spectral peak at a frequency below embedment layer frequency that is between two key frequencies, then, an additional condensation frequency should be considered. This is a must verification for soil sites with abrupt variations in layer stiffnesses with depth, as exemplified below.

The AB structure SSI analysis was performed for a highly nonuniform soil site with a shallow soft layer with  $V_s = 1,000$  fps down to 100 ft depth sitting on a much stiffer soil formation with  $V_s = 5,500$  fps.

The computed ATF (.TFU files) using the FVROM-INT approach against the reference FV method are shown in Figure 5. It should be noted that for the set of key frequencies automatically identified based on the free-field analysis, the computed SSI solution for an in-structure location at high elevation does not approximate reasonably well the 2.25 Hz ATF spectral peak. However, if the 2.25 Hz frequency is added as additional key frequency, the FV and FVROM-INT results perfectly match, as for the uniform soil case shown before.

### ***Deeply Embedded Typical SMR Structure***

The SMR structure is a RC shearwall structure with a horizontal section size of 100ft by 100ft, and a total vertical size of 162.50 ft with an embedment of 118 ft and a super-structure height above ground of 44.50 ft. The SMR SSI FE model shown in Figure 6 has a total of 30,924 nodes including 15,780 excavation nodes. The soil deposit is modeled by a uniform deep soil formation with  $V_s = 1,500$  m/s. The seismic excitation at ground surface was defined by a set of three RG1.60 spectrum compatible acceleration time histories with a maximum acceleration of 0.30g for DBE and 0.60g for BDBE. For all SSI analyses, the control motion was defined at the foundation base level.

Comparative SSI analyses were performed using FVROM-INT against the FV and Fast FV (FFV) methods. The FFV method is a refined case of the ESM method (described in ASCE 4-16) with the excavation interaction nodes being defined for all the excavation volume outer nodes plus several internal layer nodes. The SMR excavation model illustrated in Figure 7 includes 29 embedment layers, plus 2 bottom soil layers (used to ensure transition to a regular mesh for excavation). The FV excavation model includes 15,780 interaction nodes corresponding to all 30 internal node layers, while the FFV excavation model (each 2 layers skipped, w/ skip 2) includes only 7,491 interaction nodes corresponding to all excavation outer nodes plus 11 internal node layers, respectively (red dots). To simulate the embedded wall-soil interface condition shear springs were included as described in Figure 7.

Both linear and nonlinear SSI analyses were performed using FVROM-INT and the reference FV method for a maximum ground acceleration of 0.3g and 0.6g, respectively. Both structural walls and foundation-soil interface nonlinear behavior was included. Sensitivity studies were done based on US and Japan standards for nonlinear modeling of RC structures.

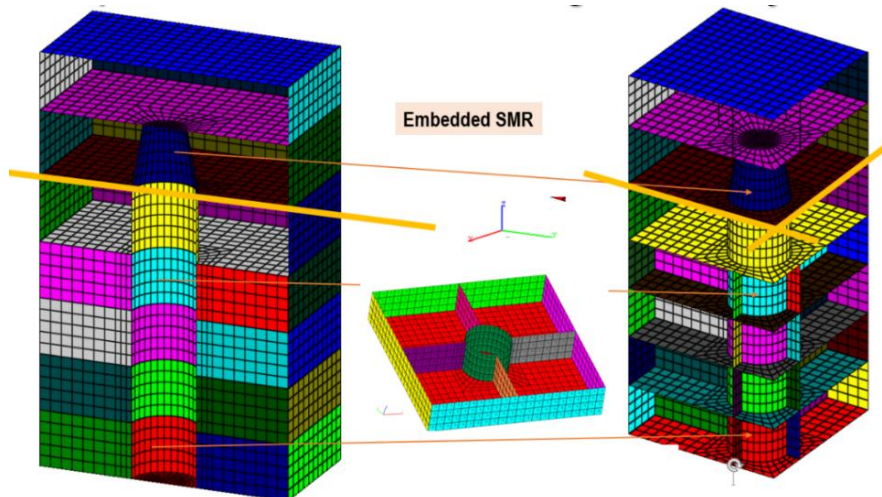


Figure 6 SMR Structure Model Description

The overall SSI analysis runtimes for FVROM-INT, reference FV method and FFV method are shown in Table 1. A regular MS Windows 10 workstation with 256 GB RAM was used for runs. Much faster runtimes can be obtained by running ACS SASSI on fast AWS cloud instances. The SSI analyses were performed for 200 SSI frequencies, while the soil impedance condensation was performed for only 20 key frequencies. For the linear SSI analysis, FVROM-INT is 8.9 times faster than reference FV method and 4.8 times faster than FFV method (w/ skip 2), while for nonlinear SSI analysis, FVROM-INT is 12.6 times faster than FV method and 6.2 times faster than FFV method (w/ skip 2).

It should be noted that FFV method (w/ skip 2) that provides highly accurate SSI responses is almost 3 times faster than reference FV method. Thus, the overall SSI runtime reduction against FV method by using FFV combined with FVROM-INT is @ 12 times for linear SSI analysis and @ 17 times for nonlinear SSI.

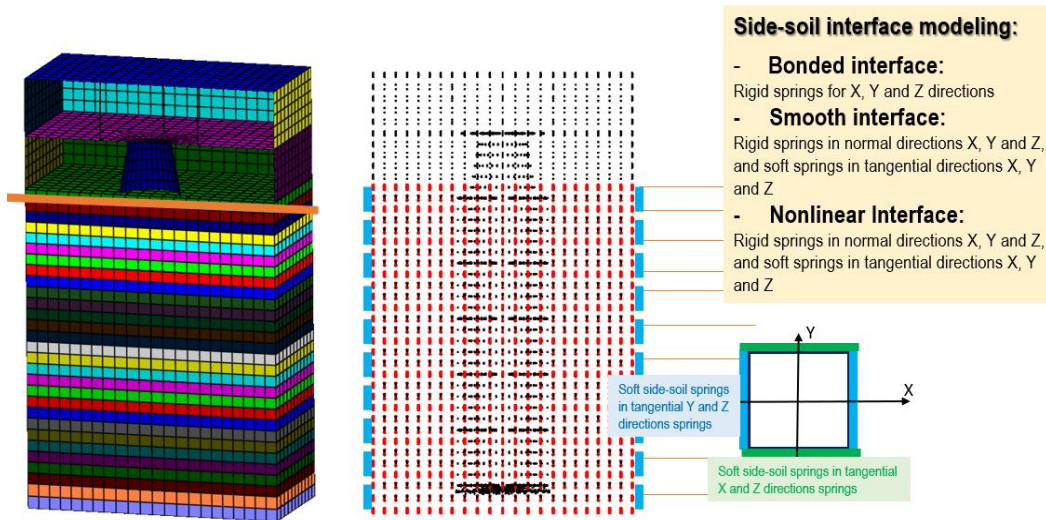


Figure 7 SMR SSI Model; FE Model Mesh (left), Nodes (middle) and Soil-Interface Modeling (right)

Table 1 Comparative SSI Analysis Runtimes Using FVROM-INT

SSI Approach	Interaction Nodes (Condensation Nodes)	Number of SSI Frequencies (Condensation Frequencies)	Linear SSI	Nonlinear SSI (5 iterations)
FV Method	15780	200	70 hours	255 hours
FVROM-INT	15780 (3081)	200 (21)	7.8 hours	20.2 hours
Speed Up Ratio	-	-	8.9 times	12.6 times

SSI Approach	Interaction Nodes (Condensation Nodes)	Number of SSI Frequencies (Condensation Frequencies)	Linear SSI	Nonlinear SSI (5 iterations)
FFV Method	7491	200	28 hours	93 hours
FVROM-INT	7491 (3081)	200 (20)	5.8 hours	15 hours
Speed Up Ratio	-	-	4.8 times	6.2 times

Figure 8 shows that the computed ATF at two SMR locations below ground surface using FVROM-INT based on FFV (w/ skip 2) against the reference FV method. Only 20 key frequencies (with square red markers) were used for impedance condensation and 200 frequencies for SSI analysis.

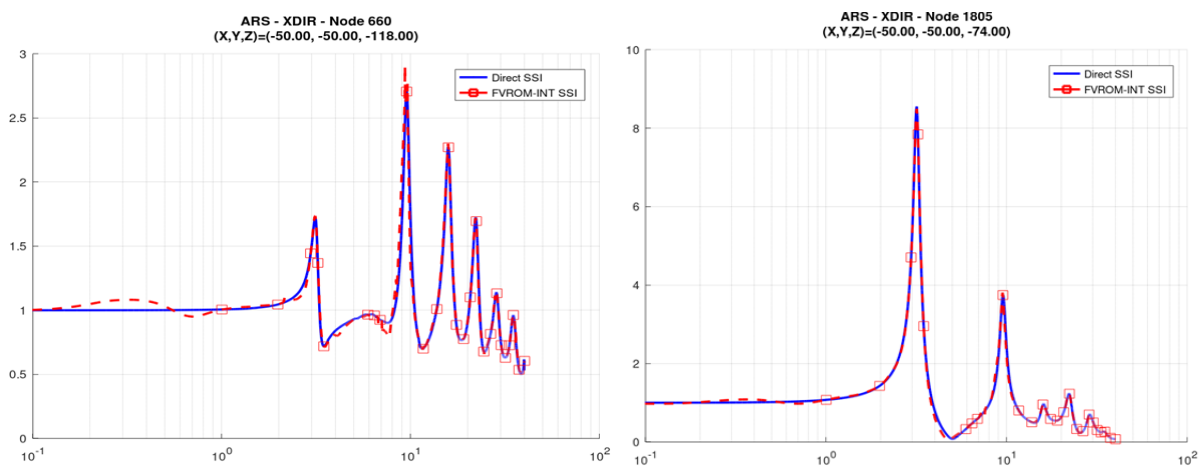


Figure 8 ATF Computed with FVROM-INT based on FFV (w/ skip 2) and Reference FV Method

The computed ISRS for the same two elevation locations are shown in Figure 9. Both the computed ATF and ISRS results indicate the high numerical accuracy of the FVROM-INT approach against the reference FV method. The FFV (w/ skip 2) provides identical results with the reference FV method for the entire range of frequency of practical interest.

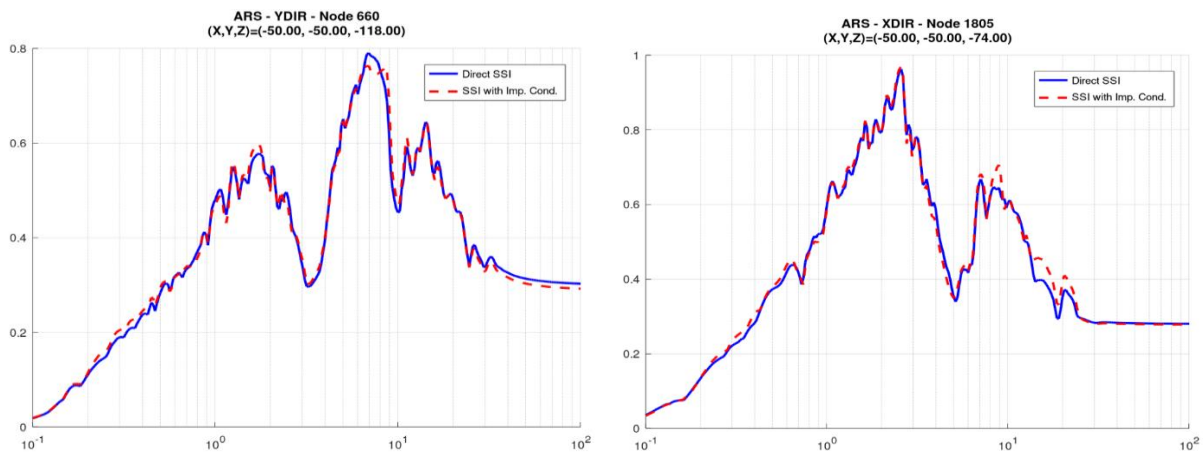


Figure 9 ISRS Computed Using FVROM-INT (“SSI with Imp. Cond.”) vs. FV Method (“Direct SSI”)

The rest of this section provides some useful engineering insights related to the deeply embedded SMR structure linear and nonlinear behavior. Sensitivity studies were performed for the wall-soil interface condition considering a smooth interface (with soft shear linear springs), a welded interface (with rigid shear linear springs) and a nonlinear interface (with nonlinear shear springs). The effects of the nonlinear SMR structure RC wall behavior and the wall-soil interface slipping were both investigated using ACS SASSI Option NON. Two ground surface seismic input levels were considered: 1) DBE Level for 0.30g and 2) BDBE level for 0.60g.

The nonlinear structure SSI analysis for 0.60g input, including both nonlinear behavior of RC walls and embedded wall-soil interface slipping convergences in 6 steps for a 10% tolerance and 8 iterations for a 5% tolerance, as shown in Figure 10 for ISRS computation. For more information on the nonlinear structure modeling, additional details are provided in two companion papers (Ghiocel et al., 2022a, b).

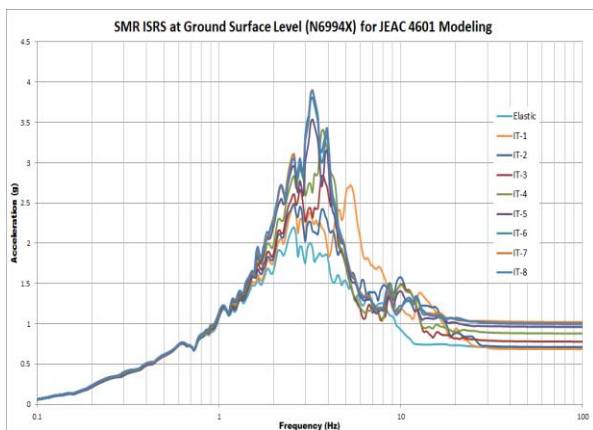


Figure 10 Computed ISRS for 8 SSI Iterations

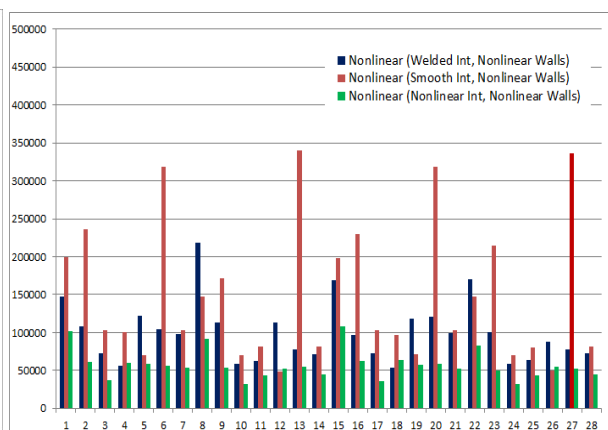


Figure 11 Interface Effects on RC Wall Stiffnesses

The effects of both the nonlinear RC wall behavior and the embedded wall-soil interface condition (welded, smooth, or nonlinear) appear to be significant for the investigated SMR structure. Figure 11 shows the effects of the wall-interface modeling on the effective RC wall in-plane stiffnesses. It should be noted that for the smooth interface condition, the effective wall stiffnesses are sensibly larger. This is due to the kinematic SSI interaction effects which are quite different for the smooth and the welded wall-soil interfaces.

Figure 12 shows the horizontal ISRS within the SMR structure at foundation level (-118 ft) and ground surface level (0 ft) for different soil interface conditions assuming either a linear or nonlinear RC wall behavior. Figure 12 results indicate that, overall, the linear SSI analysis assuming smooth interface condition and linear structure provides conservative ISRS, even overly conservative for the upper elevations of the SMR structure. The nonlinear structure behavior effects appear less significant on computed ISRS than the wall-soil interface condition effects. For the lowest elevations, both the smooth and welded conditions appear to be slightly unconservative for ISRS amplitudes in the 10-20 Hz frequency range.

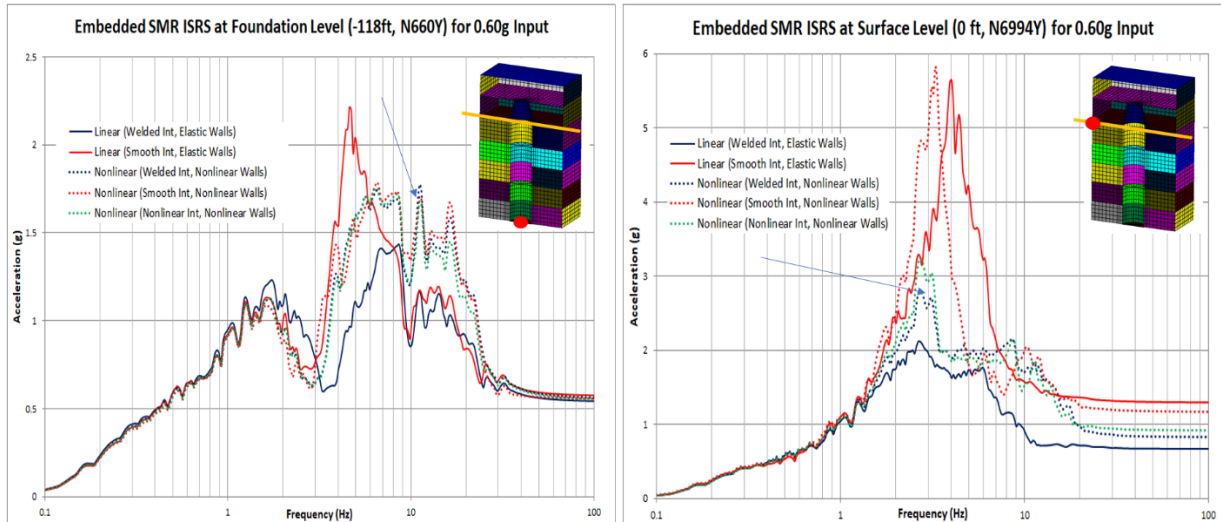


Figure 12 ISRS Computed for Different Interface Conditions for Linear or Nonlinear RC Walls

Figure 13 shows the SMR nonlinear response computed based on US (ACI 318-19, ASCE 4-16) and Japanese (JEAC 4601-2015, AIJ RC 2016) standard recommendations (Ghiocel et al, 2022a, b). Both the smooth (soft shear springs) and welded (rigid shear springs) interface conditions were included. It should be noted that for the 0.60g seismic input, the welded interface condition in comparison with the smooth interface condition produces twice larger deformation and a 30-50% force increase in the SMR structure wall at the 1<sup>st</sup> floor above ground surface. This is a result of the fact that the embedded wall is fully constrained by the dynamic soil deformation for the welded interface condition.

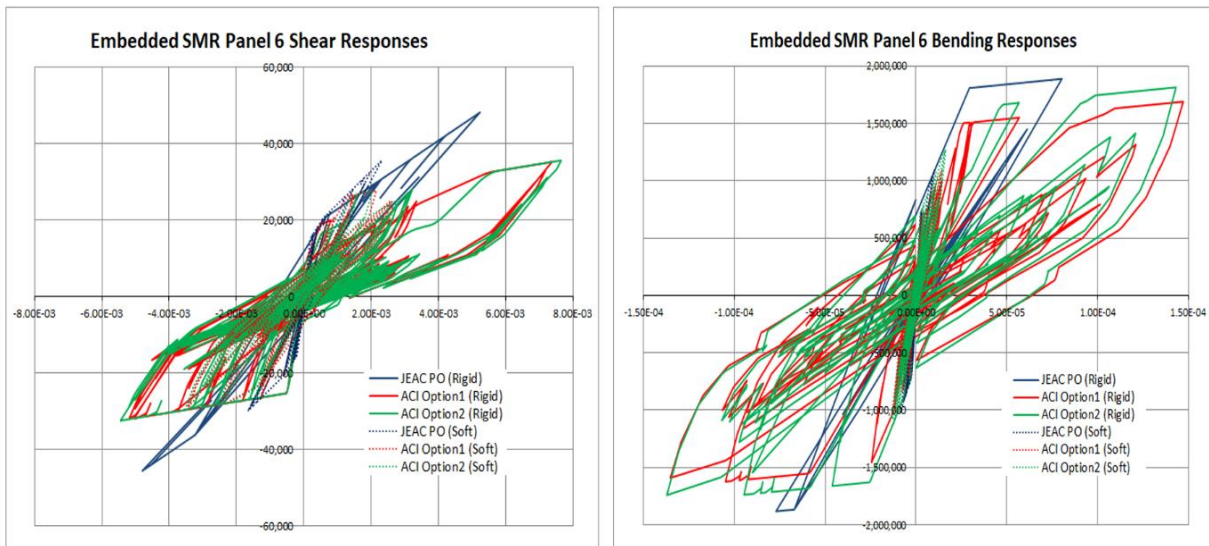


Figure 13 Shear Force (left) and Bending Moment (right) Hysteretic Responses of SMR Exterior Wall at the 1<sup>st</sup> Floor Above Ground Surface (Panel 6 in X-Direction)

Figure 14 shows the ISRS comparison at the top of SMR structure at 44.50ft elevation above ground for the same 0.60g input. There is a ISRS large amplification at the top of structure due to the nonlinear

structure behavior which appears quite surprising in comparison with ISRS computed at ground surface level. The explanation of this ISRS amplification is particular to the investigated SMR structure which includes a low-rise super-structure with a height of only 44.50m the ground surface. This significant ISRS amplification at the top of super-structure is also due to the shift of the structural fundamental frequency from about 12 Hz for the uncracked concrete walls to 3.3 Hz for the severely degraded concrete walls under the severe 0.60g input. For the 3.3 Hz frequency the dynamic amplification defined by the RG1.60 input spectrum amplitude is significantly larger for than for the 12 Hz frequency.

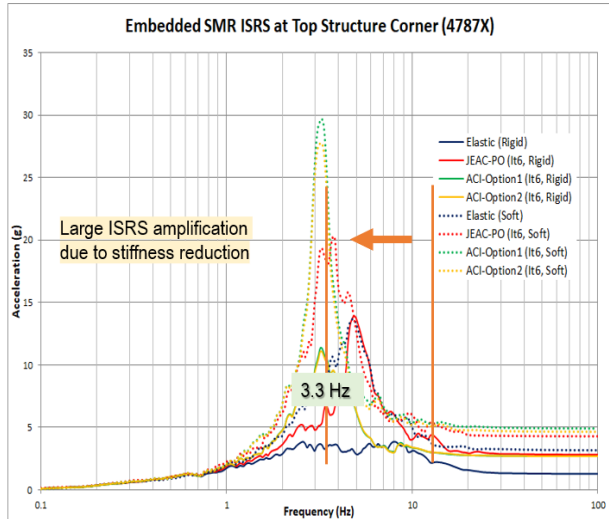


Figure 14 ISRS at Top of SMR Structure

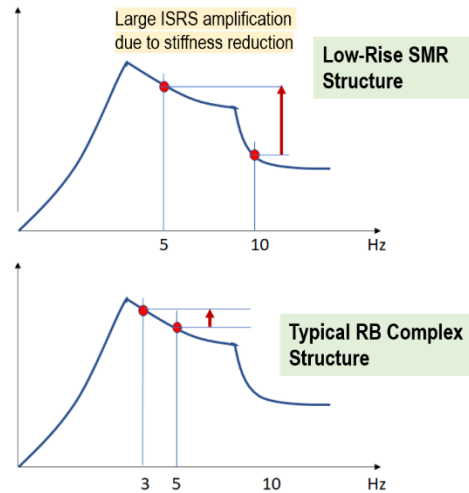


Figure 15 Frequency Shift Effect for RG1.60

Figure 15 qualitatively explains the dynamic response amplification effect due to the structure frequency shift from a higher frequency to a lower frequency for the of the investigated low-rise SMR structure (upper plot) versus a typical RB complex structure (lower plot) under RG 1.60 spectrum excitation.

The nonlinear wall-soil interface slipping was modeled using distributed shear springs with bilinear force-displacement relationships that depend on the geological static soil pressure variation with depth. The slipping forces (yielding level) correspond to the friction forces at the wall-soil interface which vary with depths up to the soil shear stress upperbound of 2 ksf (per API standard recommendation) which corresponds to a depth of about 35 ft. The nonlinear wall-soil interface slipping in the vertical direction at a 30 ft depth is shown in Figure 16 for a 0.30g input and a 0.60g input, respectively. The computed wall-soil slipping relative displacement is lower than 0.05 ft for the 0.30g input, and up to 0.15 ft for the 0.60g input. Even this slipping relative displacements are relatively small, the wall-soil interface slipping effects are visible in the SMR structure motions and forces, as illustrated in Figures 12 and 13.

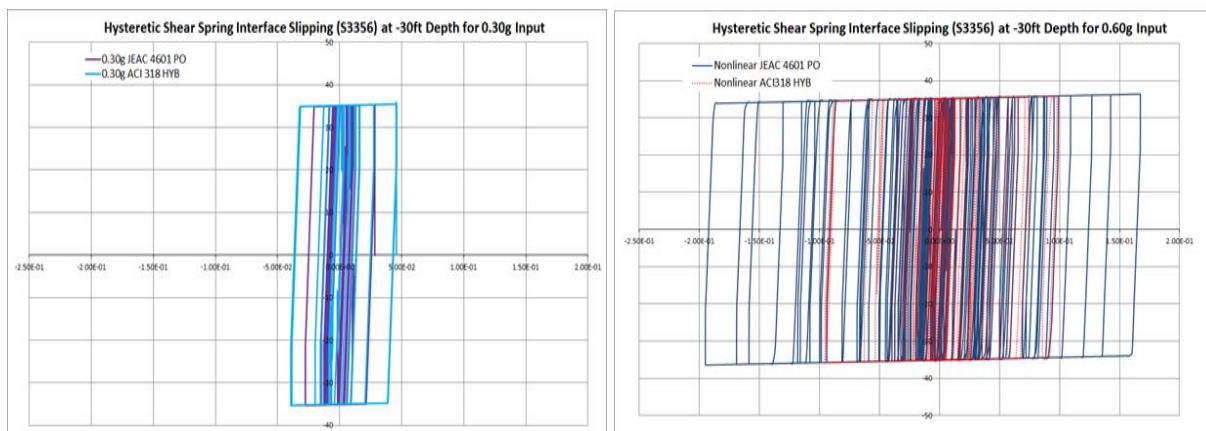


Figure 16 Wall-Soil Interface Slipping Displacement at 30ft Depth for 0.30g and 0.60g Inputs

## CONCLUDING REMARKS

The paper introduces and shows the application of the highly efficient FVROM-INT approach for seismic SSI analysis of deeply embedded structures. The FVROM-INT approach is applied to two deeply embedded structure SSI case studies including an AB shearwall structure and a typical SMR structure. Both linear and nonlinear structure SSI analyses were performed based on the FVROM-INT approach solution. It is shown that the FVROM-INT approach maintain the accuracy of SSI results, while providing large analysis speed-ups up to 12-17 times in comparison with reference FV method.

As a note of practical interest based on the investigated SMR case study is that the current seismic SSI methodologies for the SMR industry projects based on the linearized SSI analyses up to a 0.50g ground acceleration, assuming smooth and welded wall-soil interface bounding variation conditions (simulated by low and high stiffness linear shear springs, respectively) appear to be appropriate and reasonably conservative for both ISRS and structure force evaluations. For the investigated SMR structure on a uniform soil site with  $V_s=1,500$  fps, it appears that the smooth soil interface condition provides the upper bounds for ISRS, while the welded interface condition provides the upper bounds for structural story drifts and structural forces in RC walls.

The paper results provide useful insights for a better understanding of the behavior of deeply embedded SMR structures under severe earthquakes. No investigations on the non-vertically propagating seismic wave effects on SMR SSI response were included in this study. Insights on these effects are provided in a separate paper (Ghiocel, 2022).

## REFERENCES

- American Concrete Institute (2020), *Building Code Requirements for Structural Concrete and Commentary*, ACI 318-19 Standard
- American Society of Civil Engineers (2017), *Seismic Analysis for Safety-Related Nuclear Structures and Commentary*, ASCE 4-16 Standard
- ANSYS Inc. (2021). *ANSYS Engineering Simulation Software*, ANSYS Mechanical Engineering Software, Canonsburg, PA
- GP Technologies, Inc. (2021). *ACS SASSI Version 4 User Manual, Including Advanced Options A-AA, NON, PRO, RVT-SIM and UPLIFT*, Revision 5, June 15.
- Ghiocel, D.M, Nitta, Y. and R. Ikeda, T. Shono (2022a). *Seismic Nonlinear SSI Approach Based on Best Practices in US and Japan. Part 1: Modeling*, SMiRT26, Special Session on *Nonlinear Seismic SSI Analysis Based on Best Practices in US and Japan*, Berlin, July 10-15
- Ghiocel, D.M, Nitta, Y. and R. Ikeda, T. Shono (2022b). *Seismic Nonlinear SSI Approach Based on Best Practices in US and Japan. Part 2: Application*, SMiRT26, Special Session on *Nonlinear Seismic SSI Analysis Based on Best Practices in US and Japan*, Berlin, July 10-15
- Ghiocel, D.M. (2022). *Studies on Non-Vertically Seismic Wave Propagation Effects on Deeply Embedded SMR Structure Responses for Nonuniform Soils with Abrupt Stiffness Variations with Depth* SMiRT26 Conference, Division V, Berlin, July 10-15
- Ichihara, Y., Nakamura, N., Moritani, H., Horiguchi, T. and K., Choi, B. (2021). *Applicability of Equivalent Linear Analysis to Reinforced Concrete Shear Walls: 3D FEM Simulation of Experiment Results of Seismic Wall Ultimate Behavior*, Transaction of Atomic Energy Society of Japan, Advanced Publication by J-stage, doi:10.3327/taesj.J20.038
- Ichihara, Y., Nakamura, N, Nabeshima, K., Choi, B. and Nishida, A. (2022). *Applicability of Equivalent Linear Three-Dimensional FEM Analysis for Reactor Building to Seismic Response of Soil-Structure Interaction System*, SMiRT26 Conference, Special Session on *Nonlinear Seismic SSI Analysis Based on Best Practices in US and Japan*, Berlin, July 10-15
- Lysmer, J., Tabatabaie-Raissi, M., Tajirian, F., Vahdani, S., and Ostadan, F. (1981). *SASSI - A System for Analysis of Soil-Structure Interaction*, Report No. UCB/GT/81-02, Geotechnical Engineering, University of California, Berkeley, CA, April 1981.
- Mertz, G., Snyder, M., Cuesta, I., Flores, G.L., Azad, M., Watkins, D. (2019), *Improvements in Frequency Domain Soil-Structure-Fluid Interaction Analysis of Nuclear Power Plants*, SMiRT25, Division III, Charlotte, NC, August 4-9
- Nuclear Standard Committee of Japan Electric Association (2016), *Technical Code for Aseismic Design of Nuclear Power Plants, Japan Electric Association Code (JEAC 4016-2015)*